Virus-Like Particles Displaying Recombinant Short-Chain Fragment Region and Interleukin 2 for Targeting Colon Cancer Tumors and Attracting Macrophages

Virus-Like Particles Displaying Recombinant Short-Chain Fragment Region and Interleukin 2 for Targeting Colon Cancer Tumors and Attracting Macrophages

VIPIN KUMAR DEO,[1] TATSUYA KATO,[2] ENOCH Y. PARK[*,2]

[1] Laboratory of Biotechnology, College of Global-Interdisciplinary Studies, Shizuoka University, 836 Ohya, Shizuoka 422-8529, Japan

[2] Laboratory of Biotechnology, Research Institute of Green Science and Technology, Shizuoka University, 836 Ohya, Shizuoka 422-8529, Japan

[*] *Corresponding author:* Enoch Y. Park (Tel. & Fax: +81-54-238-4887; E-mail: park.enoch@shizuoka.ac.jp)

This article contains supplementary material that is available from the authors upon request or via the Internet at http://wileylibrary.com.

ABSTRACT: Functionalized virus-like particles (VLPs) can target with specificity as drug delivery systems (DDS) and can attract macrophages for the destruction of cancer cells. Here, the group antigen (gag) capsid protein from the Rous sarcoma virus was used to prepare VLPs, functionalized by displaying glycol-inositol phosphate-anchored short chain fragment region (rscFv) and hemagglutinin transmembrane region anchored recombinant human interleukin-2 (rhIL2) (designated as VLP-rscFv-rhIL2s) in silkworms. The rscFv specifically binds the tumor-associated glycoprotein 72 (TAG-72) that is expressed at the surface of colon cancer cells. VLP-rscFv-rhIL2 was affinity purified and had a smooth particle size with a diameter of 50 nm. Calcein-AM-packaged VLP-rscFv-rhIL2s successfully targeted cancer cells as a model for DDS. VLP-rscFv-rhIL2 bound with colon cancer cells that attracted macrophages (human THP-1 cells) in chemotaxis chamber assays compared to negative controls. The macrophages secreted tumor necrosis factor-α (TNF-α), a cytokine that is necessary to destroy cancer cells. These results demonstrate the potential of VLP-rscFv-rhIL2 as an intelligent nano biomaterial that is capable of attracting macrophages.

KEYWORDS: Bilayer; biomaterials; biotechnology; cancer chemotherapy; colon; nanoparticles; proteins; protein delivery; site-specific delivery; targeted drug delivery □

INTRODUCTION

Colon cancer (unresectable) is widely treated using approved chemotherapy regimens to prolong survival time by delaying tumor enlargement and increase chances to make the tumor resectable (for surgical removal).[1] The known regimens lack specificity and penetrability and have high toxicity, which limits their range of use in cancer targeting.[2] Synthetic polymer-based nanoparticles have few limitations[3]; here, we demonstrate as an alternative virus-like particles (VLPs) as a biological material that is easy to process and remove from living systems. VLPs are small (approximately 100 nm or less), with an enhanced permeation and retention effect, permitting the retention of VLPs in the near vicinity of a tumor.[4,5] In addition, VLPs, which are devoid of any genetic material, are easily detected by the immune system and cleared from the circulatory system. However, VLPs need to be functionalized to target specific cells, for gene therapy or for vaccination.

VLPs provide a surface (surrounded with or without lipid bilayer) that can be modified chemically or genetically to provide one or more additional functions to VLPs. Additional functions of VLPs, such as the ability to target or activate the innate immune system by attracting macrophages to assist in its ability to destroy its target, can be helpful. VLPs without a lipid bilayer are suitable for the covalent modification of drugs and dyes or the genetic modification of peptides onto a loop domain at the surface of a capsid protein. Such modifications lead to changes in VLPs structure, making them unstable; hence, few non-enveloped VLPs with several functions are known. In contrast, enveloped VLPs can be modified by proteins using anchors from transmembrane proteins that are easily embedded in the lipid bilayer without altering the VLP structure.

Cytokines are intermediary molecules that control the homeostasis of the immune system and have been researched as candidates for cancer immunotherapy.[6] In particular, interleukin

2 (IL-2) is a major candidate for cancer immunotherapy and has already been approved for the treatment of metastatic renal cell carcinoma and metastatic melanoma.[7] IL-2 structure and receptor studies have clearly demonstrated potential use in targeting cancer tumors.[8,9] IL-2 binds to a receptor complex of IL-2Rα, IL-2Rβ and IL-2Rγ, which are expressed on antigen-activated T-cells and natural killer cells.[10,11] IL-2 interaction with these receptors invokes responses depending on its binding affinity leading to the stimulation, motility and modulation of T-cells or NK cells.[12–14] Because IL-2 causes harmful toxicity at levels of 100 pM and above, various approaches have been devised by the fusion of IL-2 with toxins, drugs or PEGylation, but these methods still show cytotoxicity due to a lack of specificity toward the target.[13] To deliver IL-2 to cancer cells and to ameliorate the systemic toxicity of IL-2, recombinant human IL-2 (rhIL-2) fused with the antigen binding site of the anti-GD2 antibody was constructed for the treatment of human neuroblastoma tumor in a mice model.[15] This fusion protein efficiently accumulated in cancer cells, led to the induction of immune activation and slowed cancer cell growth. This cytokine proceeded to phase-I and -II trails and safely induced the immune system.[16]

Here, we are interested in Rous sarcoma virus (RSV) capsid protein gag-based VLPs that are functionalized to target colon carcinoma. rscFv specifically binds tumor-associated glycoprotein 72 (TAG-72) expressed at the surface of colon cancer cells and was displayed on the surface of RSV VLPs with rhIL2. We designed VLP-rscFv-rhIL2 such that it can target colon cancer cells, and rhIL2 can attract macrophage toward cancer cells. VLP-rscFv-rhIL2s were produced in silkworm by the co-expression of the gag, rscFv and rhIL2 proteins using *Bombyx mori* nucleopolyhedrovirus (BmNPV) bacmid. To display on the surface of RSV VLPs, rscFv and rhIL2 were anchored using glycophosphoinositol (GPI)[17] and hemagglutinin transmembrane region (HA-TM)[18], respectively. Each of these anchors can be easily embedded in a lipid bilayer to display the proteins, but here we focus on simultaneously

displaying two anchors. The VLP-rscFv-rhIL2s that were purified from silkworm larvae were evaluated by chemotaxis analysis using the colon carcinoma cell line LS174T and differentiated THP-1 cells. Our functionalized VLP-rscFv-rhIL2s would be useful not only for targeting colon cancer cells but also for attracting macrophages toward cancer cells.

MATERIALS AND METHODS

Preparation of rhIL2 Bacmid

Influenza A/California/07/2009 virus cDNA (Sino Biological VG11085-UT) (Sino Biological Inc., Beijing, China) was used to perform PCR using forward and reverse primers for HA (Table 1) to select the cDNA sequence of the transmembrane domain of hemagglutinin (HA-TM) and ligate it into the pFastBac vector by the infusion method (Takara bio, Otsu, Japan). A human placenta cDNA library was used as a template to select hIL2 cDNA using forward and reverse primers for IL2 (Table 1) and ligate it into the pFastBac vector mentioned above to produce pFastBac/rhIL2. The preparation of recombinant bacmids carrying gag- and GPI-anchored rscFvs was previously described.[17,19]

Silkworm Rearing and Bacmid Injection

Silkworm larvae were reared and fed as previously reported[17] and injected with 40 μl of recombinant bacmid DNA solutions containing 5 μg of BmNPV-gag577 bacmid,[19] 5 μg of BmNPV-rscFv bacmid,[17] and 5 μg of BmNPV-rhIL2 bacmid in 10% (v/v) DMREI-C reagent (Invitrogen, Carlsbad, CA, USA) in PBS using a 1 ml syringe with a 26G×1/2 needle (Terumo, Somerset, New Jersey, USA).

Purification of VLP-rscFv-rhIL2s and Morphology

The hemolymph containing VLP-rscFv-rhIL2s was collected and purified by affinity chromatography and confirmed by western blotting (Supplementary Information No. 1). The size of VLP-rscFv-rhIL2s was analyzed qualitatively and quantitatively by Transmission Electron Microscope (TEM) (JEM-2100F, JEOL, Ltd., Tokyo, Japan) and dynamic light scattering as previously reported.[20]

Confirmation of Anchors and Function by ELISA

The function of rscFv was confirmed by its ability to bind TAG-72 by ELISA. Human TAG-72 (Sigma, Saint Louis, Missouri, USA) at 20 U per well in 100 µl was immobilized on an immunoplate (Thermo Scientific, West Palm Beach, FL, USA) overnight at 4°C in triplicate. The protocol for ELISA was previously reported.[17] The presence of the GPI anchor was confirmed by digestion with 0.1 U of phosphatidyl-inositol specific Phospholipase C (PI-PLC) (Sigma-Aldrich) in 200 µl/well of PBS (pH 7.5) for 2 h at 27°C as previously reported.[17]

The function of rhIL2s was confirmed using 100 nanograms per well of soluble-IL-2Rα (Wako) in 100 µl of HEPES buffer pH 7.5 in triplicate incubated overnight at 4°C on an immunoplate. The plate was washed and blocked as previously reported[17], and 5 µg or 2.5 µg of VLP-rscFv-rhIL2 was added. As a negative control, 5 µg of VLP was added per well and incubated for 1 h at room temperature. The plates were washed, and 1:2,500-fold diluted mouse anti-DYKDDDDK (Medical Biological Laboratories ltd, Tokyo, Japan) in buffer was added and incubated for 1 h at room temperature. The plates were washed, and 1:5,000-fold diluted goat anti-mouse conjugated to HRP (GE Healthcare UK Ltd.) in 100 µl of buffer per well was added and incubated for 1 h at room temperature. The plates were washed, and the signal was generated as reported above.

Chemotaxis Analysis

Colon carcinoma cell line LS174T cells were used, and the cell maintenance and optimum growth conditions were similar to those previously reported.[17] THP-1 cells (Riken Cell Bank RBRC-RCB1189) were cultured with 10% (v/v) fetal bovine serum (Invitrogen) in RPMI (Life Technologies, New York, USA) at 37°C in a 5% (v/v) CO_2 incubator. THP-1 cells (1×10^5 cells per flask in 5 ml) were differentiated with 60 nM Phorbol 12-myristate 13-acetate (Sigma) and cultured for 3 days at 37°C in a 5% (v/v) CO_2 incubator. After differentiation was complete, THP-1 cells were trypsinised using TrypLE Express (Life Technologies Japan LTD., Tokyo, Japan) for 15 min at 37°C in a 5% CO_2 incubator and washed with fresh RPMI medium before use for chemotaxis experiments with a microslide IBIDI cell chamber for chemotaxis (IBIDI GmBH, Munich, Germany). The cells were washed in fresh growth medium and mixed with rat tail collagen-I (Gibco, Tokyo, Japan) as per the available IBIDI protocol with the chamber under sterile conditions. Ten micromolar of Calcein-AM (Invitrogen) and 2 μM LysoTracker Red DND-99 (Invitrogen) were loaded into differentiated macrophages and LS174T cells, respectively, by mixing the cells with dyes and incubating at 37°C in a 5% CO_2 incubator for 1 h. The excess dye was washed using fresh RPMI medium three times by centrifugation. Silica discs (Japan Vilene Company LTD., Ibaraki, Japan) were used to culture LS174T as a model (Supplementary Information No. 2) for tumors, and the ability of VLP-rscFv-rhIL2s to deliver the dyes was tested.

Macrophage Penetration of Silica Disc

Ten-thousand differentiated THP-1 cells (per flask in 5 ml) were prepared as mentioned above, loaded with 10 μM Calcein-AM (Invitrogen) and incubated for 1 h at 37°C in a 5% CO_2 incubator. The excess dye was removed by washing the cells and placed in a 35-mm glass bottom dish (Asahi Glass Co. Ltd., Tokyo, Japan). The silica disc carrying the LS174T cells

(Supplementary Information No. 2) was used and incubated at 37°C in a 5% CO_2 incubator for 3 days. After incubation, the silica disc was observed using a confocal laser-scanning microscope (LSM 700, Carl Zeiss, Oberkochen, Germany) with a 10 × lens. The image analysis was performed using the ZEN light edition software that was available with the microscope. The experiment was repeated under similar conditions to understand the penetration of macrophages. Z-stacking was performed, and Z-stacked images with a 1 μm slice were collected by confocal microscopy. The collected images were rendered using the ZEN light edition software that was available with the microscope.

ELISA and Confocal Microscope Experiment for TNF-α

VLP-rscFv-rhIL2s (10 μg per well), VLPs (10 μg per well) and hIL2 (2 μg per well) (Wako) were individually incubated with a silica disc carrying LS174T (no dyes were loaded) for 1 h. After incubation, excess was washed using the MEM-eagle medium (Sigma-Aldrich, Missouri, USA). Differentiated THP-1 cells (3×10^5 cells per well) (no dye was loaded) were seeded and incubated for 3 days. After incubation, the silica disc was washed and placed in a fresh well with fresh medium containing mouse anti-h-TNF-α (PeproTech Inc., New Jersey, USA) at a 1:750 dilution as the primary antibody and incubated for 1 h. The cells were washed thrice, and the secondary antibody A594 conjugated with rabbit anti mouse IgG (1:750 dilution) (Life Technologies, New York, USA) was added and incubated for 1 h. The cells were washed thrice, and their nuclei were stained with DAPI (4',6-diamidino-2-phenylindole) (Dojindo, Kumamoto, Japan) for 1 h at 37°C in a 5% (v/v) CO_2 incubator. Excess dye was removed by washing with fresh media and viewed under a confocal scanning laser microscope with a 10 × lens. Image analysis was performed using the ZEN light edition software that was available with the microscope.

Mouse anti-h-TNF-α (PeproTech, Inc.) at 2 μg per ml in 100 μl of HEPES buffer pH 7.5 in triplicate was added per well and incubated overnight at 4°C to coat the surface. The supernatant was discarded, washed and blocked as reported above for ELISA. The supernatant that was collected from the wells (under similar conditions as above) containing VLP-rscFv-rhIL2s, VLPs (negative control) and differentiated THP-1 cells (negative control) was added at 100 μl per well and incubated overnight at 4°C. As a positive control, 0.1 ng of TNF-α (Wako) in 100 μl of HEPES buffer (pH 7.5) was incubated overnight at 4°C in triplicate. The plates were washed, and biotinylated rabbit anti-human TNF-α (0.25 μg per ml) (PeproTech, Inc.) in 100 μl of buffer per well was added and incubated for 4 h at room temperature. The plates were washed, and 1:2,000-fold streptavidin conjugated to HRP (Invitrogen) in buffer was added and incubated for 2 h at room temperature. The plates were washed, and the signal was generated as previously reported.[18]

RESULTS

Expression, Purification and Confirmation of Display Anchors on VLP-rscFv-rhIL2

VLP-rscFv-rhIL2 was expressed and purified from the silkworm's hemolymph by affinity chromatography. The presence of gag (61 kDa), rhIL2 (19 kDa) and rscFv (32 kDa) was confirmed by western blotting (Fig. 1a–c). The gag protein showed different band due to its protease activity as previously reported, but the VLP formation was not hindered.[21]

The presence and function of rscFvs on VLP-rscFv-rhIL2s was confirmed by the affinity for TAG-72 and compared with VLPs as a negative control by ELISA (Fig. 2a). The presence of the GPI anchor was confirmed by PI-PLC enzymatic digestion (Fig. 2b) using purified VLP-rscFv-rhIL2 and VLPs. The enzymatic activity of PI-PLC specifically cleaves the phosphodiester bond, releasing rscFvs from the VLP-rscFv-rhIL2 surface and causing a

decrease in the signal intensity. rhIL2 was anchored using HA trans-membrane region, and its presence was indirectly confirmed by displaying the full-length HA protein on VLPs using TN-5B1-4 insect cells (Fig. S1a-b and Supplementary Information No. 3). A hemagglutination assay showed that functional HA is displayed on the VLPs (Fig. S1c and Supplementary Information No. 3). The display of HA is due to the transmembrane region that is present in the HA2 region.

Structural Modeling of rhIL2 and Confirmation of Function

rhIL2 structural stability in silico was calculated using internet-based I-TASSER, and models were generated (Fig. 3a–b). The generated rhIL2 model was embedded in silico in the lipid bilayer (2:1 ratio of DOPC:DOPA) using the CHARMM-GUI membrane builder software available online (www.charmm-gui.org) (Fig. 3c and Supplementary Information No. 4). The function of the lipid-layer-embedded rhIL2 on VLP-rscFv-rhIL2 was confirmed by ELISA by its specific concentration-dependent binding to the soluble IL2-Rα receptor compared to VLPs (negative control) (Fig. 3d). The confirmation of functions shows that the anchoring of rhIL2 and rscFvs was successful on VLP-rscFv-rhIL2s and did not hinder their native structure. VLP-rscFv-rhIL2 smooth morphology was confirmed qualitatively by TEM (data not shown). A quantitative assessment of the VLP-rscFv-rhIL2 diameter as performed by dynamic light scattering showed 50–80 nm, which was similar in size to VLPs[20] but smaller than VLP-rscFvs[20] (data not shown).

Chemotaxis Properties of VLP-rscFv-rhIL2s

The chemotaxis property of VLP-rscFv-rhIL2s was tested in vitro using differentiated THP-1 (macrophages) placed in an extracellular matrix made with rat tail collagen-I in an IBIDI cell chamber 1. VLP-rscFv-rhIL2s that were bound to LS174T cells (due to rscFv affinity for TAG-72) were seeded in chamber 2 (Fig. 4), whereas LS174T cells with only VLPs as a

negative control were seeded in chamber 3. The chemotaxis properties of VLP-rscFv-rhIL2 were confirmed as a significant amount of macrophages (green colored) moved out from the extracellular matrix in chamber 1 toward chamber 2 (Fig. 4a, d). The yellow color that was observed in the merged channel shows the presence of both macrophages and LS174T (Fig. 4c, f). The average movement of macrophages from chambers 1 to 2 was approximately 800 μm, as observed qualitatively, and compared to the negative control, the chemotaxis of macrophages was specifically toward colon cancer cells that were bound to VLP-rscFv-rhIL2s. Macrophages for negative control in chamber 3 showed no movement in the IBIDI cell from chambers 1 to 3 (Fig. S2b). The movement of macrophages shows the potential of VLP-rscFv-rhIL2s to attract macrophages and target tumors.

Tumor Model Using a Porous Silica Disc

A porous silica disc (average pore size 50–70 μm) serving as an exoskeleton to co-culture LS174T cells (Fig. S3) was used as a tumor model to study the penetration of macrophages and shows the delivery of dyes as a DDS model by VLP-rscFv-rhIL2. LS174T cells that were bound to VLP-rscFv-rhIL2 were loaded with LysoTracker Red, and macrophages were loaded with Calcein-AM. Based on the chemotaxis experiments using the IBIDI chamber, we hypothesized that macrophages can migrate and enter the silica disc toward LS174T cells that are bound to VLP-rscFv-rhIL2 (Fig. 5a). Calcein-AM dye shows fluorescence only when present in the cell, and the presence of both the LysoTracker Red color channel and the Calcein-AM color channel confirms the migration and penetration of macrophages into a silica disc targeting the LS174T cells (Fig. 5b–d). Under similar conditions as above, VLPs and hIL2 (negative controls) were used as they do not have rscFvs to bind to the TAG-72 marker on LS174T cells. As a result, VLPs showed no Calcein-AM fluorescence (Fig. 5e–g), but hIL2 showed a small amount of fluorescence (Fig. 5h–j). hIL2 is a small protein and, once

entrapped inside the silica pores, is difficult to remove during washes; thus, a trace amount of hIL2 causes the chemotaxis of macrophages, resulting in fluorescence.

The penetration of macrophages in the model was further analyzed by collecting 1 μm images slices using scanning laser microscope (Z-stacking) using similar conditions as above by observing the fluorescence (green and red channels) and rendering the images (Fig. 6a–b). The rendered image (Fig. 6c) shows the presence of both color channels (yellow), and the penetration is also significant.

Chemotherapy Potential of VLP-rscFv-rhIL2s

LS174T cells (stained with DAPI) when mixed with VLP-rscFv-rhIL2s attracted macrophages to secrete TNF-α, as shown by the fluorescence using mouse anti-TNF-α (Fig. 7a–c). As a negative control under similar conditions, VLPs and hIL2 were each mixed with colon cancer cells (stained with DAPI), and no fluorescence was observed for VLPs (Fig. 7d–f). A small amount of TNF-α secretion was detected with hIL2 (Fig. 7g–i) due to the inability to remove the non-specifically bound hIL2. TNF-α secretion observed with VLP-rscFv-rhIL2-treated cells was more than that observed with hIL2-treated cells, demonstrating the specificity and effectiveness of the therapy model. Under similar conditions as above, the supernatant was collected, and the TNF-α secretion by macrophages was confirmed by sandwich ELISA results compared to the negative control (Fig. 7j). The TNF-α secretion that was observed with VLP-treated cells and differentiated THP-1 cells was less than that with VLP-rscFv-rhIL2s.

DISCUSSION

A multifunctional nano biomaterial clubbed with DDS platforms providing the precise targeting and effective delivery of drugs to tumors is greatly needed. We propose that gag-

protein-derived VLPs can fulfill the multifunctional DDS platforms criteria. Here, multifunctional VLPs were rationally designed to display different proteins on their surface using suitable anchors independent of each other (Fig. 2a–b) as each protein is guided toward the plasma membrane by its own signal. The displayed proteins have specific functions; rscFvs target tumor-specific TAG-72 marker proteins, and rhIL2 binds to specific receptors, such as IL-2Rα (Fig. 3d), indicating that VLPs can themselves act as empty cages delivering dyes and drugs to tumors as a model for therapy.

To treat tumors effectively, a quick and effective immune system, along with use of drugs that actively destroy tumors, is needed. Only the immune system by itself or drugs against tumors cannot fully resolve the tumor problem. Nanoparticle-derived medicines have shown success in vitro and in vivo against cancer, but they passively target using an enhanced permeability and retention effect and require adjuvants to be presented to antigen presenting cells.[22] Here, we have developed active nanoparticles without adjuvants that specifically target TAG-72 so that this approach can target metastatic cancer in different places. To reinforce cytotoxicity to cancer cells, chemotherapeutic drugs, other cytokines and peptide vaccines have been combined with IL-2 for cancer immunotherapy.[6,7] VLP-rscFv-rhIL2 can bind to LS174T cells and attract the activated macrophages (Fig. 4a–d). The activated macrophages moved toward a silica disc harboring VLP-rscFv-rhIL2s bound to LS174T cells and penetrated the disc that was used as a tumor model. The macrophages secreted TNF-α (Fig. 7a–c), a known cytokine for therapy against cancers that plays an important role in the regulation of immune cells.[13] The interior of VLP is empty; therefore, we previously demonstrated that RSV VLPs can be packaged with drugs or dyes[17,18], indicating that the chemotherapeutic drugs cisplatin and dacarbazine can be packaged into RSV VLP-rscFv-rhIL2 and that dual-functional chemotherapeutic agents can be created. In the case of RSV VLP-rscFv-rhIL2 having chemotherapeutic drugs, these drugs can also be specifically

delivered to cancer cells expressing TAG-72, mitigating the side effects of chemotherapeutic drugs.

CONCLUSION

We demonstrated that VLPs can display rhIL2 and rscFv proteins using HA-TM and GPI anchors, respectively, as a model. Each of the anchors was different and assembled on VLPs efficiently producing VLP-rscFv-rhIL2s, providing VLPs with two new functions of targeting and attracting macrophages toward colon cancer cells. The efficient use of two or more anchors can permit the display of more proteins on VLPs, making VLP-based DDS platform more versatile. The ability to attract macrophages in a silica disc as a tumor model shows that other components of the innate immune system could also be activated by their display on VLPs. This hypothesis needs to be tested in vitro and using mice for the future development of this platform.

ASSOCIATED CONTENT

Supplementary Information

Experimental details for the purification and confirmation of VLP-rscFv-rhIL2; Silica disc carrying LS174T cells as a tumor model; Display of full-length HA on VLP; hemagglutination assay and its confirmation. Figure S1, Expression of VLP-HA in insect cells, and the hemagglutination assay and its confirmation; Figure S2, Microscopic observation of LS174T cells and macrophages with VLPs as a negative control for the chemotaxis experiment; Figure S3, Silica disc carrying LS174T cells. This material is available free of charge via the internet at http://pubs.acs.org.

Notes

The authors declare no competing financial interest.

ACKNOWLEDGMENTS

We thank Prof. Hiroshi Ueda and Associate Prof. Tomohiro Suzuki of the Tokyo Institute of Technology and Utsunomiya University for providing the scFv plasmid and for providing the expertise on Linux OS for simulations, respectively. We wish to thank Ms. Megumi Yui for carrying out the plasmid preparation for HA-TM that was used in the current work.

REFERENCES

1. Watanabe T, Itabashi M, Shimada Y, Tanaka S, Ito Y, Ajioka Y, Hamaguchi T, Hyodo I, Igarashi M, Ishida H, Ishiguro M, Kanemitsu Y, Kokudo N, Muro K, Ochiai A, Oguchi M, Ohkura Y, Saito Y, Sakai Y, Ueno H, Yoshino T, Fujimori T, Koinuma N, Morita T, Nishimura G, Sakata Y, Takahashi K, Takiuchi H, Tsuruta O, Yamaguchi T, Yoshida M, Yamaguchi N, Kotake K, Sugihara K. 2012. Japanese Society for Cancer of the Colon and Rectum (JSCCR) Guidelines 2010 for the treatment of colorectal cancer. Int J Clin Oncol 17 (1): 1–29.
2. Maksimenko A, Alami M, Zouhiri F, Brion J-DD, Pruvost A, Mougin J, Hamze A, Boissenot T, Provot O, Desmaële D, Couvreur P. 2014. Therapeutic modalities of squalenoyl nanocomposites in colon cancer: An ongoing search for improved efficacy. ACS Nano 8 (3): 2018–32.
3. Pokorski JK, Steinmetz NF. 2011. The art of engineering viral nanoparticles. Mol Pharm 8 (1): 29-43.
4. Goerner M, Seiwert TY, Sudhoff H. 2010. Molecular targeted therapies in head and neck cancer—an Update of recent developments. Head Neck Oncol *2*:8.
5. Bertrand N, Wu J, Xu X, Kamaly N, Farokhzad OC. 2014. Cancer nanotechnology: The impact of passive and active targeting in the era of modern cancer biology. Adv Drug Delivery Rev 66: 2–25.

6. Lee S, Margolin K. 2011. Cytokines in cancer immunotherapy. Cancers 3(4): 3856–3893.
7. Sim GC, Radvanyi L. 2014. The IL-2 cytokine family in cancer immunotherapy. Cytokine Growth Factor Rev 25(4): 377–390.
8. Taniguchi T, Matsui H, Fujita T, Takaoka C, Kashima N, Yoshimoto R, Hamuro J. 1983. Structure and expression of a cloned cDNA for human interleukin-2. Nature 302 (5906): 305–310.
9. Boder ET. 2012. Protein engineering: Tighter ties that bind. Nature 484 (7395): 463–464.
10. Rao BM, Girvin AT, Ciardelli T, Lauffenburger DA, Wittrup KD. 2003. Interleukin-2 mutants with enhanced α-receptor subunit binding affinity. Protein Eng 16 (12): 1081–1087.
11. Wang X, Rickert M, Garcia CK. 2005. Structure of the quaternary complex of interleukin-2 with Its α, β, and γ_c receptors. Science 310 (5751): 1159–1163.
12. Teodorczyk-Injeyan JA, Sparkes BG, Lalani S, Peters WJ, Mills GB. 1992. IL-2 regulation of soluble IL-2 receptor levels following thermal injury. Clin Exp Immunol 90: 36–42.
13. Vazquez-Lombardi R, Roome B, Christ D. 2013. Molecular engineering of therapeutic cytokines. Antibodies 2 (3): 426–451.
14. Bergström SE, Bergdahl E, Sundqvist KG. 2013. A cytokine controlled mechanism for integrated regulation of T lymphocyte motility, adhesion and activation. Immunology 140 (4): 441–455.
15. Sabzevari H, Gillies SD, Mueller BM, Pancook JD, Reisfeld RA. 1994. A recombinant antibody-interleukin 2 fusion protein suppresses growth of hepatic human neuroblastoma metastases in severe combined immunodeficiency mice. Proc Natl Acad Sci USA 91(20): 9626–9630.

16. Hank JA, Gan J, Ryu H, Ostendorf A, Stauder MC, Sternberg A, Albertini M, Lo K-MM, Gillies SD, Eickhoff J, Sondel PM. 2009. Immunogenicity of the hu14.18-IL2 immunocytokine molecule in adults with melanoma and children with neuroblastoma. Clin Cancer Res 15(18): 5923–5930.
17. Deo VK, Yui M, Alam J, Yamazaki M, Kato T, Park EY. 2014. A model for targeting colon carcinoma cells using single-chain variable fragments anchored on virus-like particles via glycosyl phosphatidylinositol anchor. Pharm Res 31 (8): 2166–2177.
18. Kato T, Yui M, Deo VK, Park EY. 2015. Development of Rous sarcoma virus-like particles displaying hCC49 scFv for specific targeted drug delivery to human colon carcinoma cells. Pharm Res 32: 3699–3707.
19. Deo VK, Yoshimatsu K, Otsuki T, Dong J, Kato T, Park EY. 2013. Display of Neospora caninum surface protein related sequence 2 on Rous aarcoma virus-derived gag protein virus-like particles. J Biotechnol 165 (1): 69–75.
20. Deo VK, Kato T, Park EY. 2015. Chimeric virus-like particles made using GAG and M1 capsid proteins providing dual drug delivery and vaccination platform. Mol Pharm 12 (3): 839–845.
21. Xiang Y, Ridky TW, Krishna KN, Leis J. 1997. Altered Rous sarcoma virus gag polyprotein processing and its effects on particle formation. J Virol 71 (3): 2083–2091.
22. Shao K, Singha S, Clemente-Casares X, Tsai S, Yang Y, Santamaria P. 2015. Nanoparticle-based immunotherapy for cancer. Nano 9 (1): 16–30.
23. Yang J, Yan R, Roy A, Xu D, Poisson J, Zhang Y. 2015. The I-TASSER Suite: Protein structure and function prediction. Nat Methods 12 (1): 7–8.
24. Roy A, Kucukural A, Zhang Y. 2010. I-TASSER: A unified platform for automated protein structure and function prediction. Nat Protoc 5 (4): 725–738.

25. Klauda JB, Venable RM, Freites JA, O'Connor JW, Tobias DJ, Mondragon-Ramirez C, Vorobyov I, MacKerell AD, Pastor RW. 2010. Update of the CHARMM all-atom additive force field for lipids: Validation on six lipid types. J Phys Chem B: 114 (23): 7830–7843.

26. Dwyer PJ, Vander Valk RJ, Caltaldo V, Demianicz D, Kelty SP. 2014. All-atom CHARMM force field and bulk properties of perfluorozinc phthalocyanines. J Phys Chem A: 118 (49): 11583–11590.

Figure Legends

Figure 1. Western blot analysis of purified VLP-rscFv-rhIL2s. Purified VLP-rscFv-rhIL2s were loaded onto 5~20% supersep^{TM} ace SDS-PAGE gels (Wako). Lane 1: MagicMark^{TM} XP (Invitrogen), Lanes 2 and 3: 1 μg and 0.5 μg per lane of VLP-rscFv-rhIL2s, respectively. (a) gag-577 (61 kDa) detected using a rabbit polyclonal anti-gag primary antibody against RSV-gag-577. (b) rhIL2 (19 kDa) detected using a goat polyclonal anti-IL2 primary antibody. (c) rscFv (32 kDa) detected using a mouse monoclonal anti-DYKDDDDK primary antibody against the DYKDDDDK tag.

Figure 2. Confirmation of specificity of the displayed proteins and their anchoring. (a) The specificity of rscFvs for TAG-72 on purified VLP-rscFv-rhIL2s was confirmed by ELISA. $^{*}p > 0.05$. (b) GPI anchors of rscFvs on VLP-rscFv-rhIL2a were confirmed by ELISA using PI-PLC enzymatic digestion with (black bars) and without (white bars) PI-PLC. $^{*}p > 0.05$.

Figure 3. Structural analysis of rhIL2 anchored to Has, and the VLP-rscFv-rhIL2 size distribution. (a) rhIL2 viewed using PyMOL molecular viewer. Green is rhIL2, and yellow is the transmembrane region of HA2. Blue is the N-terminus and red is the C-terminus of rhIL2. The white dashed line shows the proposed structure buried region in the lipid bilayer. (b) The table showing the various scores from I-TASSER for model-1.[23,24] (c) Embedded rhIL2 in the lipid bilayer (2:1 ratio of DOPC:DOPA) as viewed using PyMOL molecular viewer and the protein.[25,26] (d) rhIL2 specificity for soluble IL-R α using VLP-rscFv-rhIL2s (white bars) and VLPs only (grey bar). Data are the mean ± standard deviation (n = 3). $^{*}p > 0.05$.

Figure 4. Chemotaxis properties of VLP-rscFv-rhIL2s. Confocal laser-scanning microscope images of 3×10^5 THP-1 cells (macrophages) that were loaded with Calcein-AM (green color) in chamber 1 (dotted line in right panel) and 1.35×10^6 LS174T cells that were loaded with

LysoTracker Red (red color) in chambers 2 and 3. The LS174T cells in chamber 2 were mixed with 10 μg of VLP-rscFv-rhIL2s. (a and d) IBIDI μ-SLIDE chamber 2 image showing the green fluorescence of Calcein-AM. (b and e) LysoTracker-Red-stained LS174T cells. Merged images of all the color channels (c and f). Black arrows point to the boundary (white dotted lines) between chambers 1 and 2. Scale bars are 50 μm.

Figure 5. Chemotaxis in the porous silica disc tumor model. LS174T cells were loaded with LysoTracker Red (red color) and treated with VLP-rscFv-rhIL2s (10 μg), VLPs (10 μg) and hIL2 (2 μg), whereas 1×10^5 macrophage cells were loaded with Calcein-AM dye (green). (a) Schematic representation of the set up with the silica disc in a 35 mm glass-bottomed dish for chemotaxis. (b–d) VLP-rscFv-rhIL2s, (e–g) VLPs as a negative control and (h–j) hIL2 mixed with LS174T cells. (b, e and h) Calcein-AM-loaded macrophages cells, (c, f and i) LysoTracker-Red-loaded LS174T cells and (d, g and j) DIC merged with color channels. Scale bars are 50 μm.

Figure 6. Penetration of macrophages in a porous silica disc as a tumor model. VLP-rscFv-rhIL2s (10 μg) with LS174T cells and 1×10^5 macrophage cells were loaded with LysoTracker Red dye (red) and Calcein-AM dye (green), respectively. Z-stacked images with 1 μm slices were collected and rendered using Carl-Zeiss software. (a) Red indicates the LS174T cells; (b) green from Calcein-AM indicates the macrophages; (c) merged (yellow) shows the penetration of macrophages.

Figure 7. Chemotherapy potential of VLP-rscFv-rhIL2s. VLP-rscFv-rhIL2s (10 μg) with LS174T cells in a 4-mm-diameter silica disc were incubated with 3×10^5 macrophage cells. LS174T cells with VLP-rscFv-rhIL2s (10 μg) (a–c), VLPs (10 μg) (d–f) and hIL2 (2 μg) (g–i) were stained with DAPI (a, d and g) and detected with mouse anti-TNF-α as the primary antibody and rabbit anti mouse IgG conjugated with A594 (b, e and h). DIC merged with

438 color channels (c, f and i). Scale bars are 50 μm. (j) Detection of TNF- α by sandwich ELISA

439 using the supernatant that was collected from experiments under similar conditions as above.

440 Data are the mean ± standard deviation (n = 3). $^{*}p > 0.05$.

441

442 **Table 1.** List of primers that were used to select IL-2 cDNA and to clone the HA-TM region.

Name	5’ to 3’
Forward primer for HA	CGGGGTACCATGGACTACAAGGATGACGATGAC AAGATGAAGGCAAACCTACTGGT
Reverse primer for HA	TCCCCGCGGTCAGATGCATATTCTGCACT
pFastBac vector forward primer	TCGAGGCATGCGGTACCAAGCTTGTCGAG
pFastBac vector reverse primer	AATTCCGCGCGCTTCGGACCGGGATC
Forward primer for IL2	AATGAATTCATGTACAGGATGCAACTCCT
Reverse primer for IL2	ATACTAGTTCAAGTCAGTGTTGAGATGA

443

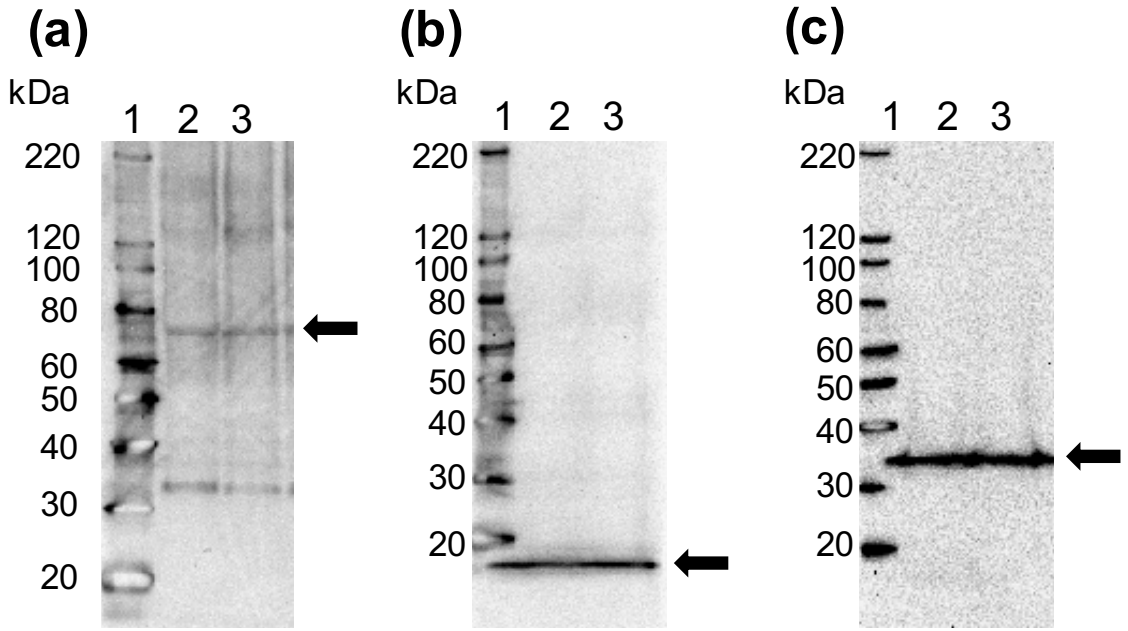
(a)
kDa
1 2 3
220
120
100
80
60
50
40
30
20
(b)
kDa
1 2 3
220
120
100
80
60
50
40
30
20
(c)
kDa
1 2 3
220
120
100
80
60
50
40
30
20

Figure 2, Deo et al.,

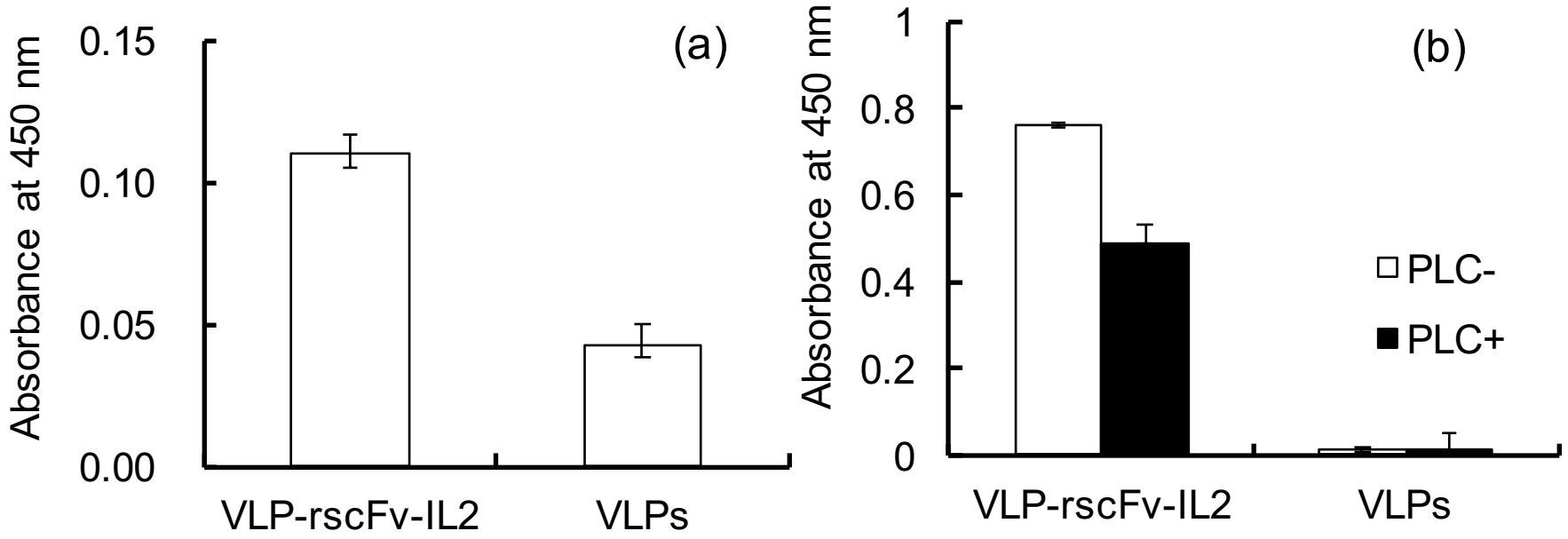

(a)

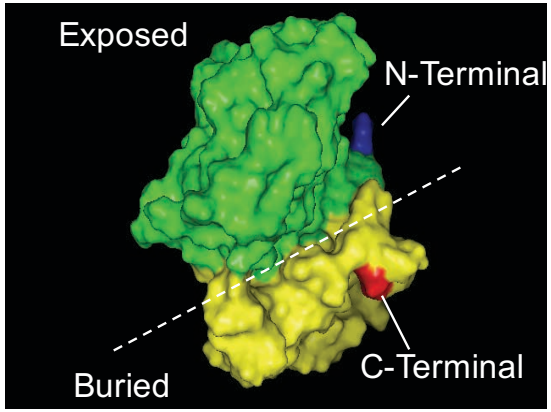

(c)

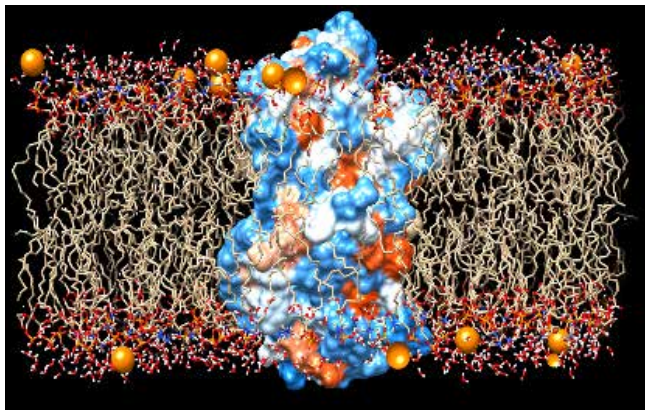

(b)

Name	Model 1
C-score	-2.70
Exp. TM-score	0.40±0.14
Exp. RMSD	11.8±4.5
No. of decoys	1646
Cluster density	0.0242

(d)

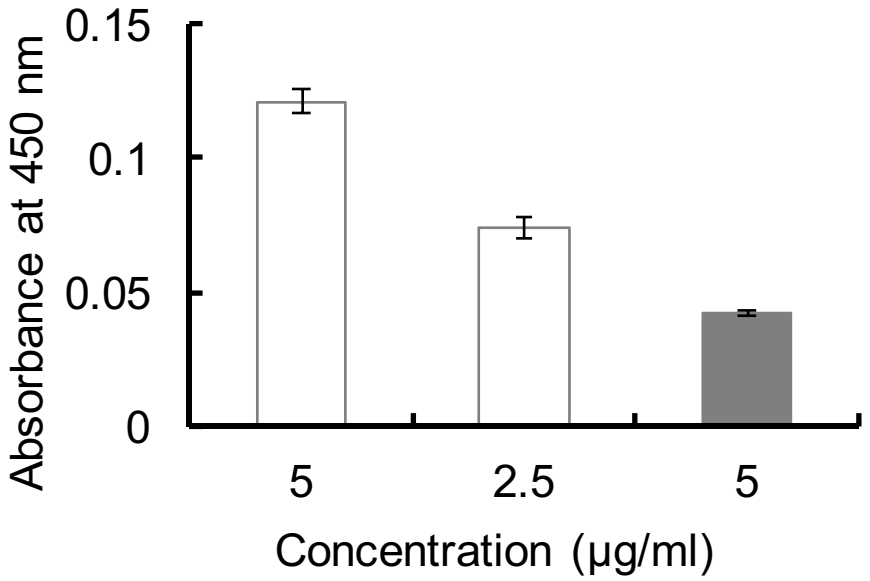

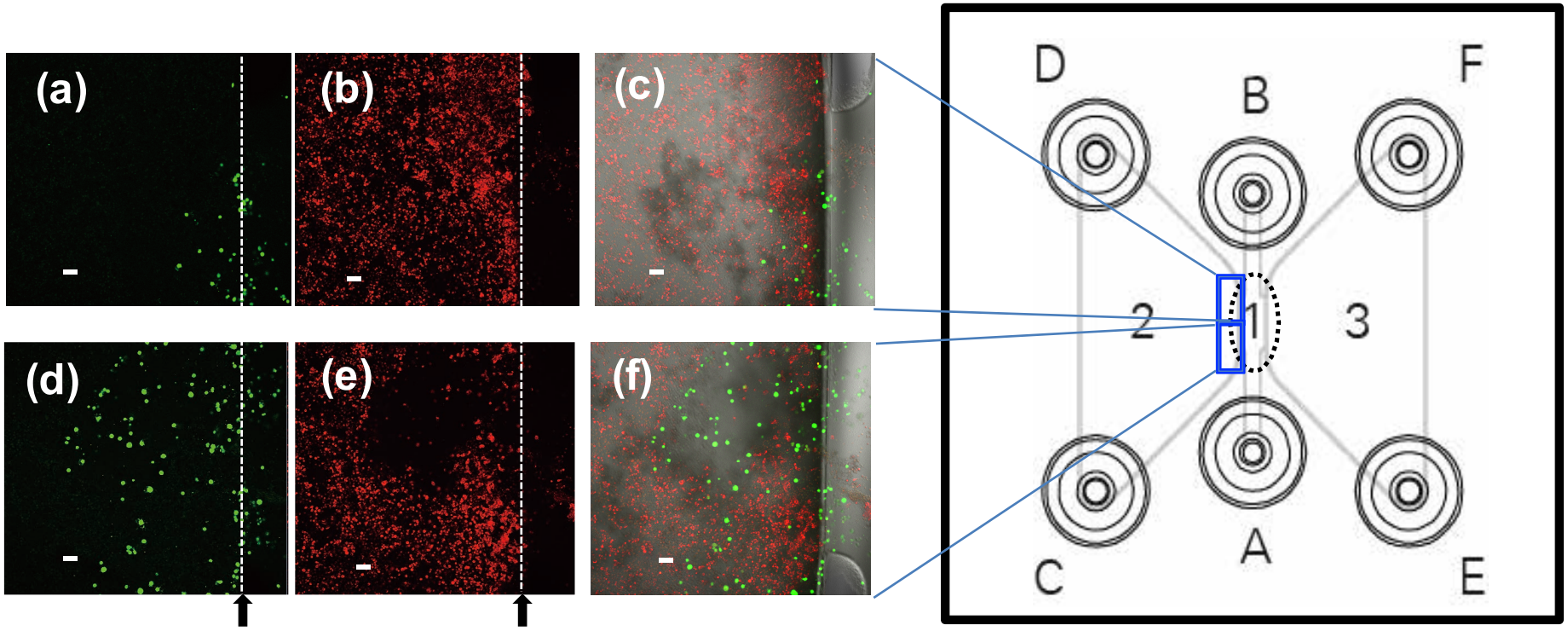
(a)
(b)
(c)
(d)
(e)
(f)
D
B
F
2
1
3
C
A
E

Figure 5, Deo et al.,

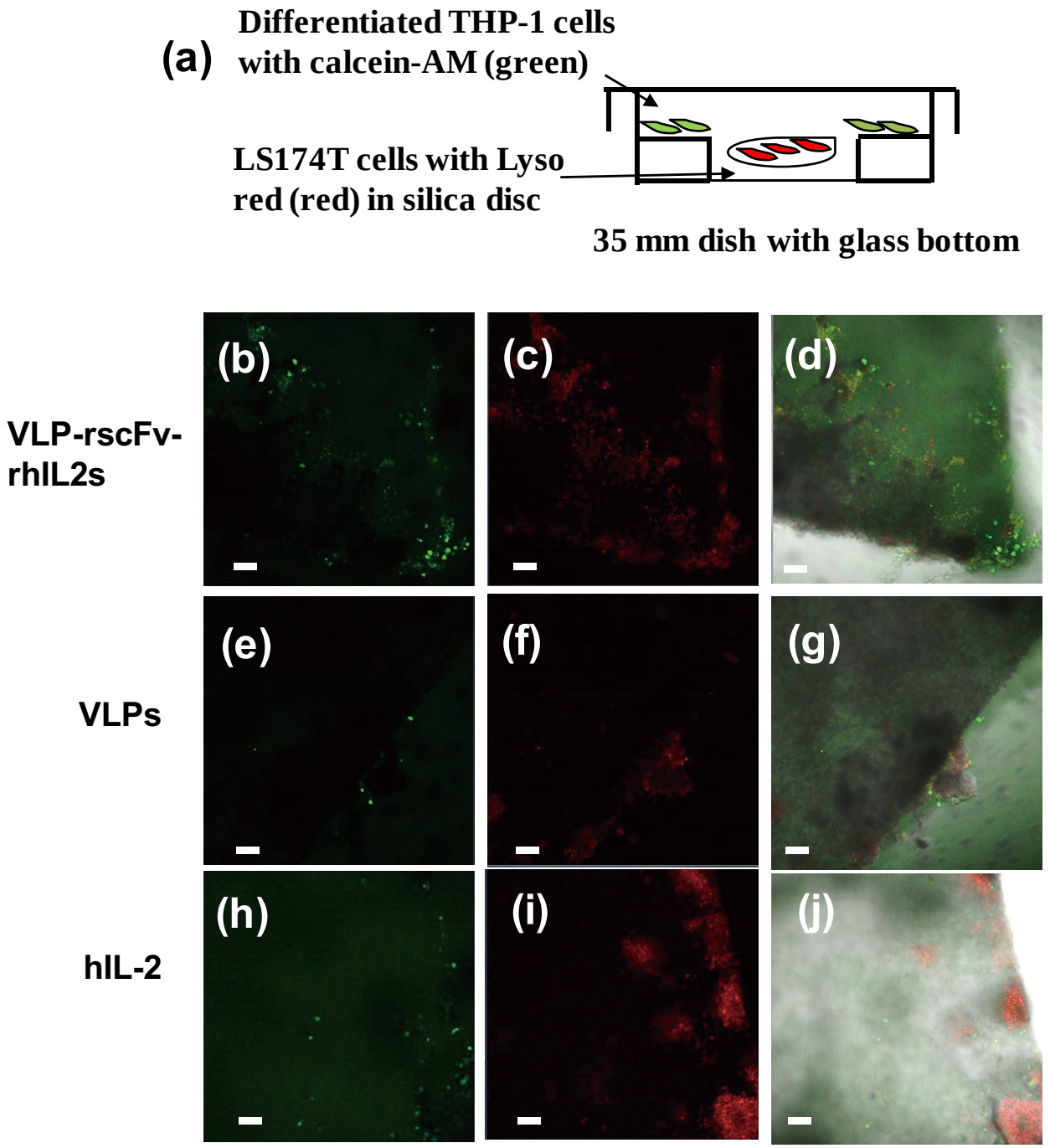

Figure 6, Deo et al.,

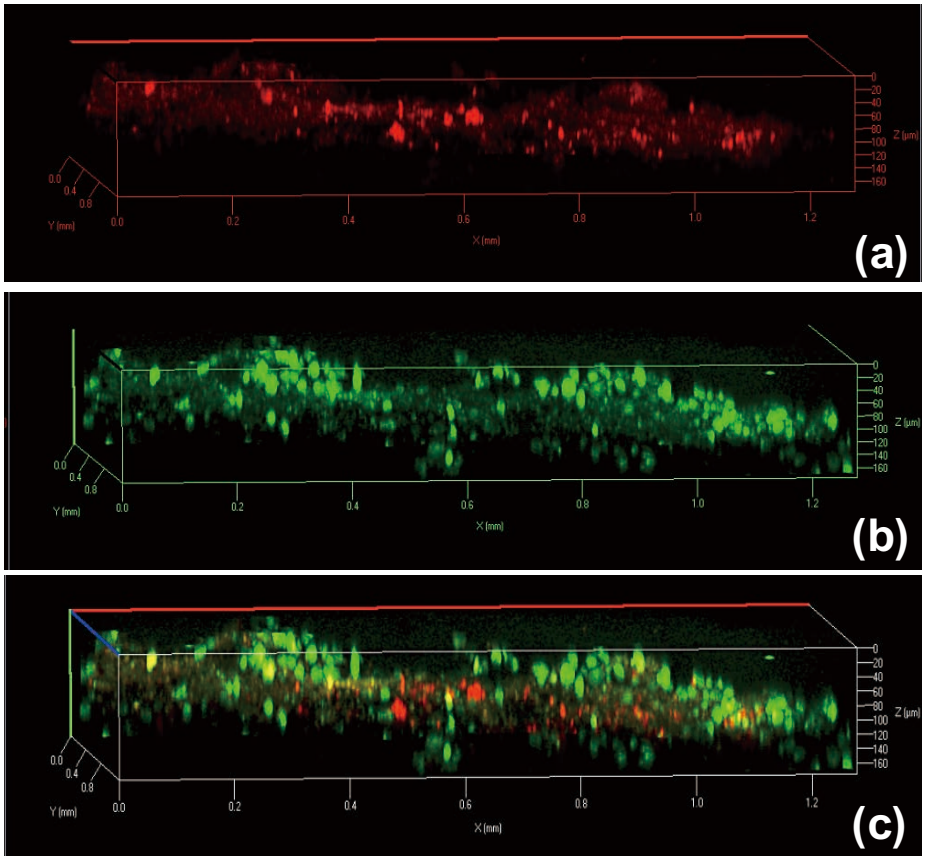

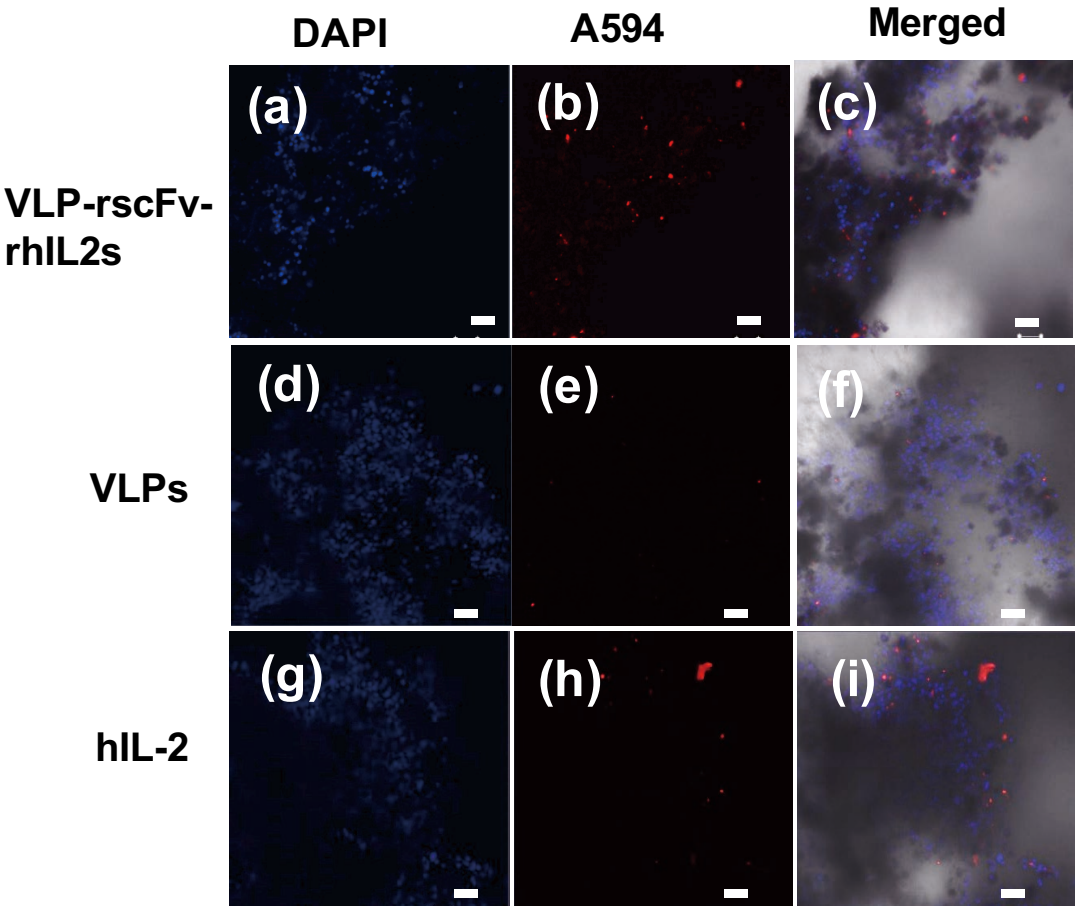
DAPI
A594
Merged
(a)
(b)
(c)
VLP-rscFv-rhIL2s
(d)
(e)
(f)
VLPs
(g)
(h)
(i)
hIL-2

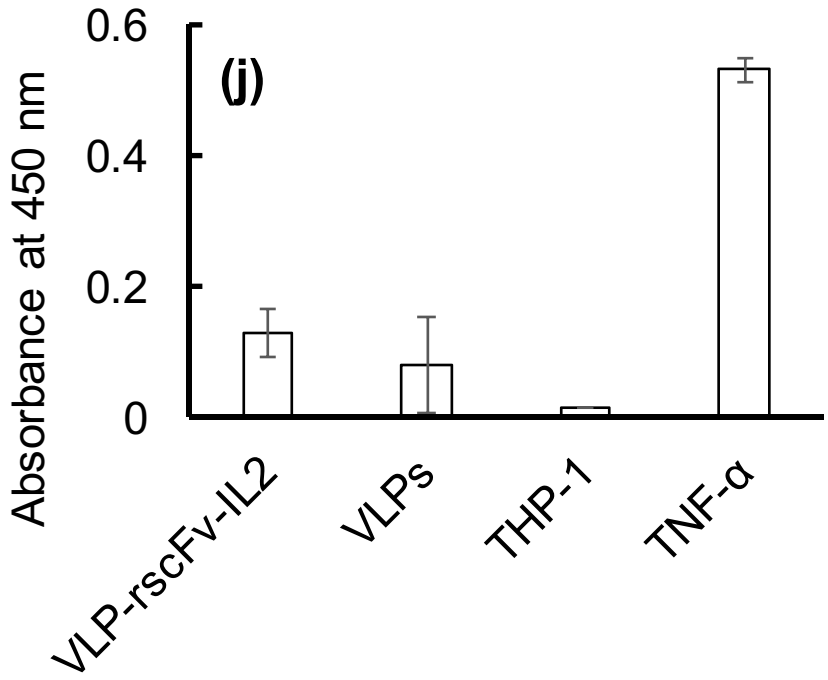
(j)
Absorbance at 450 nm
0.6
0.4
0.2
0
VLP-rscFv-IL2
VLPs
THP-1
TNF-α

Supplementary Information

Virus Like Particles Displaying Recombinant Short Chain Fragment Region and Interleukin 2 for Targeting Colon Cancer Tumors and Attracting Macrophages

VIPIN KUMAR DEO,[1] TATSUYA KATO,[2] ENOCH Y. PARK[1,2]

[1] Laboratory of Biotechnology, College of Global-Interdisciplinary Studies, Shizuoka University, 836 Ohya, Shizuoka 422-8529, Japan

[2] Laboratory of Biotechnology, Research Institute of Green Science and Technology, Shizuoka University, 836 Ohya, Shizuoka 422-8529, Japan

[1] *Correspondence to:* Enoch Y. Park (Tel. & Fax: +81-54-238-4887; E-mail: park.enoch@shizuoka.ac.jp)

This article contains supplementary material available from the authors upon request or via the Internet at http://wileylibrary.com.

(Supplementary information for Materials and Methods)

1. ***Purification and confirmation of VLP-rscFv-rhIL2***

2. ***Silica disc carrying LS174T cells as a tumor model***

3. ***Display of full length HA on VLP, hemagglutination assay and its confirmation***

4. ***Analysis of rhIL2 by I-TASSER and CHARMM-GUI (membrane builder)***

1. Purification and confirmation of VLP-rscFv-rhIL2

Hemolymph containing VLP-rscFv-rhIL2s was collected from 30 silkworms and dialyzed with cellulose ester dialysis membrane (Spectrum Laboratories Inc., California, USA) having 300,000 Da molecular weight cut off in 2 L of HEPES buffer (pH 7.5) overnight at 4°C. The purification was performed using DDDDK-agarose gel as per kit protocol. The purified protein was aliquoted and kept at -20°C. Purified VLP-rscFv-rhIL2s were loaded onto 5~20% supersep^{TM} ace SDS-PAGE gels (Wako Pure Chem. Ind. Ltd., Osaka, Japan) using ATTO II-300 system (ATTO Co., Tokyo, Japan). After SDS-PAGE, proteins were blotted on to a PVDF membrane using the Mini Trans-Blot Electrophoretic Transfer cell (Bio-Rad) at 15 V for 1 hour. The membrane was probed for gag, rhIL2 and rscFv using rabbit polyclonal anti-RSV-gag for gag-577 at 5,000 fold dilution,[1] goat polyclonal anti-IL2 (abcam, Tokyo, Japan) at 2 µg per ml and mouse monoclonal anti-DYKDDDDK[2] (Wako) at 3,000 fold dilutions, respectively. The membrane was incubated for 2 hour at room temperature. The membrane was washed thrice with TBST and incubated with mouse anti-rabbit IgG conjugated with HRP (Santa Cruz Biotechnology, Santa Cruz, California, USA), donkey anti-goat IgG conjugated with HRP (Abcam) and rabbit anti-mouse IgG conjugated with HRP (Santa Cruz Biotechnology) respectively for 2 hour at room temperature. The membrane was washed thrice

and bands were detected using immobilon western blotting reagent pack (Millipore Corporation, Billerica, Massachusetts, USA) and Fluor-S MAX Multi Imager (Bio-Rad).

2. Silica disc carrying LS174T cells as a tumor model

Silica disc (Japan Vilene company Ltd., Ibaraki, Japan) (thickness 200 μm and average pore size 50 μm) allows the growth of cells were cut under sterile conditions in 4 mm diameter and kept in 1 ml of RPMI growth medium overnight at 37°C. The following day 5,000 LS174T cells were added and incubated for 2–3 weeks with change in media every 4th day. To count number of LS174T cells in silica disc is difficult owing to the porous three dimensional structure. The silica disc was monitored after media change under light microscope and based upon the cell growth visible from the surface the silica disc were used for further experiment.

Silica disc with LS174T cells were grown as mentioned in above sections and loaded with LysoRed tracker DND-99 (2 μM) (Invitrogen, Tokyo, Japan) for 1 hour at 37°C in 5% CO2 incubator. The excess dye was washed with fresh medium change and the cells were used for experiments. VLP-rscFv-rhIL2s (10 μg per well), VLPs (10 μg per well) and hIL2 (2 μg per well) (Wako), respectively were incubated with silica disc carrying LS174T for 1 hour at 37°C in 5% CO2 incubator.

3. Display of full length HA on VLP, hemagglutination assay and its confirmation

Using primers (Table 1) hemagglutinin (HA) cDNA was isolated by PCR from pDP122B (ATCC® 39736™). HA (A/PR/8/34) cDNA was cloned into pIZ/V5-Dest Gateway vector (Invitrogen, California, USA) and used for stable expression in insect cell expression system. The co-transfection of pIZ/V5-HA-Dest, screening and stable cell lines producing HA and RSV-gag-577 was done as per protocol previously reported.[1] D6/HA cell line suspension

culture was scaled up to 2 L and the supernatant containing HA displaying VLP (VLP-HA) was collected under sterile conditions.

The stably expressing D6/HA 10,000 cells were observed using confocal laser microscope (LSM 700, Carl Zeiss, Oberkochen). Cells were fixed on glass slide (2 × 2 cm) and blocked with 5% BSA (w/w), washed and incubated with mouse primary anti-FLAG (Sigma-Aldrich, Montana, USA) for 2 hour at room temperature. The cells were washed again and incubated with Cy3 labelled anti-IgG secondary antibody for 2 hour at room temperature before being viewed under microscope.

The supernatant collected was concentrated using KVICK start cassette with 100 kDa molecular weight cutoff (GE Healthcare Amersham Biosciences KK, Tokyo, Japan). The purified protein was used for hemagglutination assay and confirmation of the VLP-HA by TEM and immuno-TEM. The rabbit erythrocytes (Nihon BioTest Research, Tokyo, Japan) washed in PBS were seeded 10% (v/v) per well. Purified VLP-HA was 2-fold serially diluted in rabbit erythrocytes to determine the hemagglutination. VLP only and PBS pH 7.5 only were used as negative control. The size of VLP-HA was analyzed qualitatively by TEM as reported earlier.[2]

4. Analysis of rhIL2 by I-TASSER and CHARMM-GUI (membrane builder)

Human IL2 (PDB no. 1m47) amino acid sequence in frame with HA-trans-membrane region was used to generate the rhIL2 model structure using I-TASSER. The amino acid sequence in FASTA format was uploaded on the website and the output data as model1 in pdb format was generated. The model1 pdb file was subsequently used to embed in a lipid bilayer composed of DOPC and DOPA in 2:1 ratio using CHARMM-GUI (membrane builder) as per the protocol

77 available on their website.[3–6] The output data in pdb format was visualized using pymol
78 molecular viewer (PyMOL Molecular Graphics System, Ver. 1.7.2.1 Schrödinger, LLC.).

79 **References**

80 (1) Deo VK, Tsuji Y, Yasuda T, Kato T, Sakamoto N, Suzuki H, Park EY. 2011. Expression
81 of an RSV-Gag Virus-like Particle in Insect Cell Lines and Silkworm Larvae. J Virol
82 Methods, 177 (2), 147–152.
83 (2) Deo VK, Yoshimatsu K, Otsuki T, Dong J, Kato T, Park EY. 2013. Display of Neospora
84 Caninum Surface Protein Related Sequence 2 on Rous Sarcoma Virus-Derived Gag Protein
85 Virus-like Particles. J Biotechnol, 165 (1), 69–75.
86 (3) Jo S, Kim T, Iyer VG, Im W. 2008. CHARMM-GUI: A Web-Based Graphical User
87 Interface for CHARMM. J Comput Chem, 29 (11), 1859–1865.
88 (4) Jo S, Kim T, Im W. 2007. Automated Builder and Database of Protein/membrane
89 Complexes for Molecular Dynamics Simulations. PLoS ONE, 2 (9), e880.
90 (5) Wu EL, Cheng X, Jo S, Rui H, Song KC, Dávila-Contreras EM, Qi Y, Lee J, Monje-
91 Galvan V, Venable RM, Klauda JB, Im W. 2014. CHARMM-GUI Membrane Builder toward
92 Realistic Biological Membrane Simulations. J Comput Chem, 35 (27), 1997–2004.
93 (6) Jo S, Lim JB, Klauda JB, Im W. 2009. CHARMM-GUI Membrane Builder for Mixed
94 Bilayers and Its Application to Yeast Membranes. Biophys J, 97 (1), 50–58.

95

(Supplementary Information for Figures)

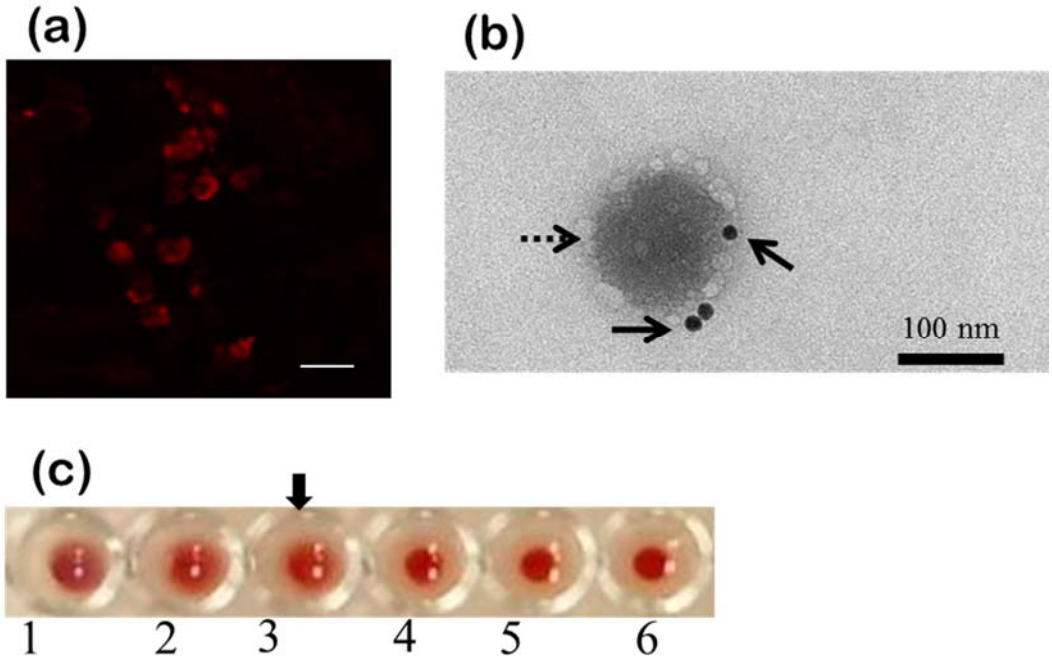

Figure S1. Expression of VLP-HA in insect cells and hemagglutination assay and its confirmation. (a) Observation of HA display in VLP-HA in insect cell line D6/HA probed with mouse anti-FLAG antibody and goat anti mouse anti IgG conjugated with Cy3. Scale bar is 50 μm. (b) VLPs/HA was confirmed by immuno electron microscopy using mouse anti-DYKDDDDK and rabbit anti-mouse IgG conjugated with 10 nm gold particle. Solid arrows show HA, Dot arrows show the lipid bilayer surrounding VLPs. (c) Hemagglutination assay was performed using rabbit reticulocytes. From 1st well up till 3rd well (2^{-2}) hemagglutination is observed and from the following well the reticulocytes settle down.

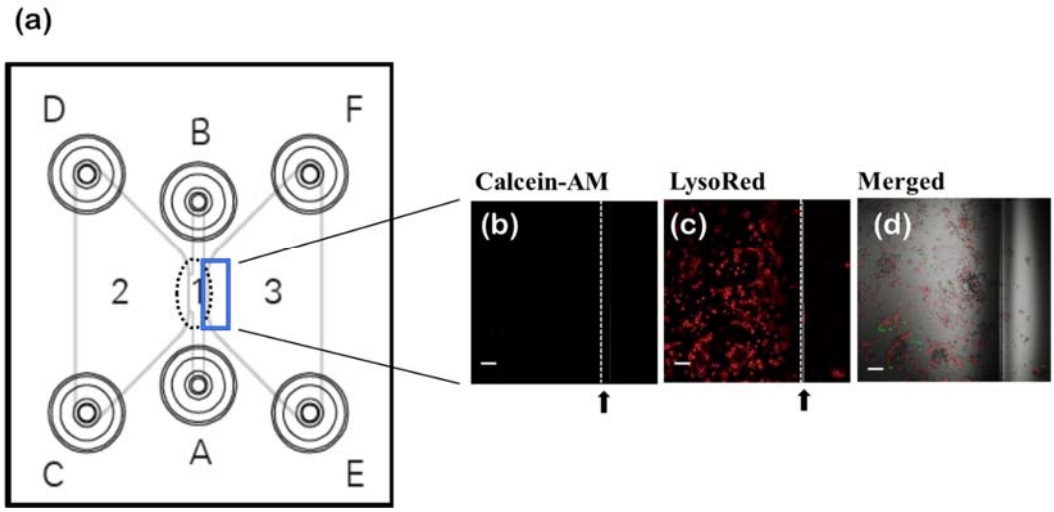

Figure S2. Microscopic observation of LS174T cells and macrophages with VLPs as negative control for chemotaxis experiment. Confocal laser scanning microscope pictures of 1×10^5 macrophages cells loaded with calcein-AM (green color) in chamber 1and 1.35×10^6 LS174T cells loaded with lyso-red dye (red color) in chamber 2 and 3 respectively. LS174T cells in chamber 2 only were mixed with 10 μg VLP as negative control (a–c). (a) Schematic diagram of IBIDI chamber used for chemotaxis. (b) IBIDI chamber 2 image showing no green color channel fluorescence of calcein-AM. (c) lyso-red stained LS174T cells. (d) Merged images of all the color channels. Black arrows in b and c point to boundary (white lines) between chamber 1 and 2. Scale bars are 50 μm.

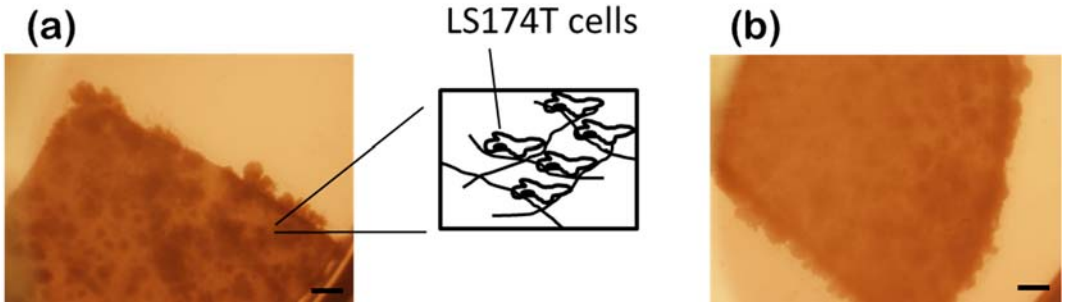

Figure S3. Silica disc carrying LS174T cells. (a) LS174T cultured in silica disc for 2 weeks under light microscope. Inset is the schematic representation. (b) LS174T cultured in silica disc for 3 weeks under light microscope. Scale bars are 20 μm.